

Is There Asymmetry Between the Concave and Convex Pedicles in Adolescent Idiopathic Scoliosis? A CT Investigation

Colin M. Davis BSc, MBBS, Caroline A. Grant PhD, Mark J. Pearcy DEng,
Geoffrey N. Askin FRACS, Robert D. Labrom MSc, FRACS, Maree T. Izatt BPhy,
Clayton J. Adam PhD, J. Paige Little PhD

Received: 22 June 2016 / Accepted: 21 November 2016 / Published online: 29 November 2016
© The Association of Bone and Joint Surgeons® 2016

Abstract

Background Adolescent idiopathic scoliosis is a complex three-dimensional deformity of the spine characterized by deformities in the sagittal, coronal, and axial planes. Spinal fusion using pedicle screw instrumentation is a widely used method for surgical correction in severe (coronal deformity, Cobb angle $> 45^\circ$) adolescent idiopathic scoliosis curves. Understanding the anatomic difference in the pedicles of patients with adolescent idiopathic scoliosis is essential to reduce the risk of neurovascular or visceral injury through pedicle screw misplacement.

Each author certifies that he or she, or a member of his or her immediate family, has no funding or commercial associations (eg, consultancies, stock ownership, equity interest, patent/licensing arrangements, etc) that might pose a conflict of interest in connection with the submitted article.

All ICMJE Conflict of Interest Forms for authors and *Clinical Orthopaedics and Related Research*® editors and board members are on file with the publication and can be viewed on request.

Each author certifies that his or her institution approved the protocol for this investigation and all investigations were conducted in conformity with ethical principles of research. The use of the historical CT dataset for research purposes was ethically approved separately by the hospital and university ethics committees.

Electronic supplementary material The online version of this article (doi:10.1007/s11999-016-5188-2) contains supplementary material, which is available to authorized users.

C. M. Davis (✉), C. A. Grant, M. J. Pearcy, G. N. Askin,
R. D. Labrom, M. T. Izatt, C. J. Adam, J. P. Little
Paediatric Spine Research Group, Institute of Health and
Biomedical Innovation at Centre for Children's Health Research,
Queensland University of Technology, Brisbane, Australia
e-mail: Colin.davis@uqconnect.edu.au

C. M. Davis, C. A. Grant, M. J. Pearcy, G. N. Askin,
R. D. Labrom, M. T. Izatt, C. J. Adam, J. P. Little
Mater Health Services, South Brisbane, Australia

Questions/Purposes To use CT scans (1) to analyze pedicle anatomy in the adolescent thoracic scoliotic spine comparing concave and convex pedicles and (2) to assess the intra- and interobserver reliability of these measurements to provide critical information to spine surgeons regarding size, length, and angle of projection.

Methods Between 2007 and 2009, 27 patients with adolescent idiopathic scoliosis underwent thoracoscopic anterior correction surgery by two experienced spinal surgeons. Preoperatively, each patient underwent a CT scan as was their standard of care at that time. Twenty-two patients (mean age, 15.7 years; SD, 2.4 years; range, 11.6–22 years) (mean Cobb angle, 53° ; SD, 5.3° ; range, 42° – 63°) were selected. Inclusion criteria were a clinical diagnosis of adolescent idiopathic scoliosis, female, and Lenke type 1 adolescent idiopathic scoliosis with the major curve confined to the thoracic spine. Using three-dimensional image analysis software, the pedicle width, inner cortical pedicle width, pedicle height, inner cortical pedicle height, pedicle length, chord length, transverse pedicle angle, and sagittal pedicle angles were measured. Randomly selected scans were remeasured by two of the authors and the reproducibility of the measurement definitions was validated through limit of agreement analysis.

Results The concave pedicle widths were smaller compared with the convex pedicle widths at T7, T8, and T9 by 37% ($3.44 \text{ mm} \pm 1.16 \text{ mm}$ vs $4.72 \text{ mm} \pm 1.02 \text{ mm}$; $p < 0.001$; mean difference, 1.27 mm; 95% CI, 0.92 mm–1.62 mm), 32% ($3.66 \text{ mm} \pm 1.00 \text{ mm}$ vs $4.82 \text{ mm} \pm 1.10 \text{ mm}$; $p < 0.001$; mean difference, 1.16 mm; 95% CI, 0.84 mm–1.49 mm), and 25% ($4.10 \text{ mm} \pm 1.57 \text{ mm}$ vs $5.12 \text{ mm} \pm 1.17 \text{ mm}$; $p < 0.001$; mean difference, 1.02 mm; 95% CI, 0.66 mm–1.39 mm), respectively. The concave pedicle heights were smaller than the convex at T5 ($9.43 \text{ mm} \pm 0.98$ vs $10.63 \text{ mm} \pm 1.10 \text{ mm}$; $p = 0.002$; mean difference,

1.02 mm; 95% CI, 0.59 mm–1.45 mm), T6 (8.87 mm \pm 1.37 mm vs 10.88 mm \pm 0.81 mm; $p < 0.001$; mean difference, 2.02 mm; 95% CI, 1.40 mm–2.63 mm), T7 (9.09 mm \pm 1.24 mm vs 11.35 mm \pm 0.84 mm; $p < 0.001$; mean difference, 2.26 mm; 95% CI, 1.81 mm–2.72 mm), and T8 (10.11 mm \pm 1.05 mm vs 11.86 mm \pm 0.88 mm; $p < 0.001$; mean difference, 1.75 mm; 95% CI, 1.30 mm–2.19 mm). Conversely, the concave transverse pedicle angle was larger than the convex at levels T6 (11.37° \pm 4.48° vs 8.82° \pm 4.31°; $p = 0.004$; mean difference, 2.54°; 95% CI, 1.10°–3.99°), T7 (12.69° \pm 5.93° vs 8.65° \pm 3.79°; $p = 0.002$; mean difference, 4.04°; 95% CI, 1.90°–6.17°), T8 (13.24° \pm 5.28° vs 7.66° \pm 4.87°; $p < 0.001$; mean difference, 5.58°; 95% CI, 2.99°–8.17°), and T9 (19.95° \pm 5.69° vs 8.21° \pm 4.02°; $p < 0.001$; mean difference, 4.74°; 95% CI, 2.68°–6.80°), indicating a more posterolateral to anteromedial pedicle orientation.

Conclusions There is clinically important asymmetry in the morphologic features of pedicles in individuals with adolescent idiopathic scoliosis. The concave side of the curve compared with the convex side is smaller in height and width periapically. Furthermore, the trajectory of the pedicle is more acute on the convex side of the curve compared with the concave side around the apex of the curve. Knowledge of these anatomic variations is essential when performing scoliosis correction surgery to assist with selecting the correct pedicle screw size and trajectory of insertion to reduce the risk of pedicle wall perforation and neurovascular injury.

Introduction

Adolescent idiopathic scoliosis is a complex three-dimensional (3-D) deformity of the spine characterized by abnormal development in the sagittal, coronal, and axial planes. The deformity is present in 2% to 4% of children between the ages of 10 and 16 years [23]. If left untreated, there is a small potential for this deformity to progress to the point where it can cause pain, abnormal posture, and very rarely, impaired cardiorespiratory function [34]. Posterior spinal fusion using pedicle screw instrumentation is a widely used method for surgical correction in progressive and/or severe adolescent idiopathic scoliosis curves, with multiple studies reporting on the curve correction achieved, the desired levels to include in the fusion, the incidence of implant complications, and long-term deformity correction outcomes compared with other surgical approaches to correct adolescent idiopathic scoliosis [2, 4, 8, 17, 26, 27].

Although newly developed imaging navigation techniques can assist in improving pedicle screw placement, failure to select appropriate screw size, screw starting point, and screw trajectory can result in pedicle screw

misplacement which potentially can cause serious neurologic, vascular, or visceral injury [9, 10, 12, 29, 32]. There have been numerous studies examining the morphologic features of the pedicle and placement of pedicle screws in normal and adolescent idiopathic scoliosis spines using various definitions and measuring modalities [18, 25, 30, 31, 35, 36]. The majority of these studies have identified clear size asymmetry in the pedicle widths between the concave and convex sides of the curve. However, clear knowledge gaps or inconsistent findings exist regarding the rest of the morphologic features of the pedicle including pedicle height and the angle of orientation of the pedicles in the axial and the sagittal planes. This study aims to clarify these knowledge gaps and inconsistencies by looking at the pedicles in patients with adolescent idiopathic scoliosis more comprehensively and with a more clinically relevant and reliably reproducible measurement method. Through the use of a historical set of CT scans of patients with preoperative adolescent idiopathic scoliosis, we (1) compared the pedicle anatomy between the concave and convex pedicles and (2) assessed the intra- and interobserver reliability of these measurements methods.

Patients and Methods

Between 2007 and 2009 a total of 27 patients with adolescent idiopathic scoliosis were surgically treated by two experienced spinal surgeons (GNA and RDL). In the weeks before thoracoscopic anterior scoliosis correction surgery, every patient underwent a low-dose CT scan as was the routine standard of care at that time to ensure safer screw sizing [11]. Twenty-two patients (81%) (Table 1) were selected for analysis in the current study based on inclusion criteria of (1) a clinical diagnosis of adolescent idiopathic scoliosis, (2) female, and (3) Lenke type 1 adolescent idiopathic scoliosis [14] with the major curve confined to the thoracic spine (Table 2). Reasons for exclusion of five patients were: (1) male, (2) major curve was not confined to the thoracic spine, (3) insufficient data, (4) Lenke type 4 adolescent idiopathic scoliosis, and (5) hemivertebrae. All Cobb [6] angle measurements, Risser grading [22], and Lenke classifications were performed by two highly experienced spinal orthopaedic surgeons (GNA and RDL) who subsequently performed the surgery. The selection criteria used was adapted from a previous study by our research group [19]. The historical CT databank had ethical approval for use in research from our hospital and university ethics committees.

Scans were performed from T1 to S1 with the patient in the supine position on Brilliance 64 (Phillips Healthcare, Amsterdam, Netherlands) or LightSpeed[®] VCT (GE

Table 1. Demographics of the study cohort

Demographics (n = 22 patients)	Average	Range	Standard deviation
Age (years)	15.7	11.6–22	2.5
Weight (kg)	56.3	37.5–84.7	12.2
Major Cobb angle (°)	53.3	42–63	5.3
Number of spinal levels in major curve	7.1	5–9	0.9

Table 2. Frequency of curve apex levels in the study cohort

Apex level	Number
T7	1
T7/8	4
T8	2
T8/9	7
T9	3
T9/10	5

Healthcare, Buckinghamshire, UK) machines with X-ray source voltage of 80 to 120 kVP. The source current range was 29 to 65 mA for all scans, with the exception of one scan in which the operator inadvertently did not follow the low-dose protocol, resulting in a source current of 119 mA. The voxel dimensions of the scans were between $0.49 \times 0.49 \times 1.00$ mm and $0.78 \times 0.78 \times 1.25$ mm. Dose reports were commissioned for both scanners with the highest estimated radiation dose of 3.0 mSv occurring with the GE Light-Speed® VCT scanner, with uncertainties owing to the dose model on the order of $\pm 20\%$. Estimated radiation doses for the Phillips Brilliance 64-slice CT scanner were substantially lower on the order of 2.0 mSv [24]. By comparison, the combined dose for posteroanterior and lateral standing radiographs is approximately 1.0 mSv, and the annual background radiation in Queensland, Australia is approximately 2.0 mSv. The scans were measured using the imaging software AMIRA 5.5.0 (FEI, Hillsboro, OR, USA).

Image Processing

Each CT scan was opened using AMIRA with synchronized axial, coronal, and sagittal displays. The image contrast levels were standardized to enable clear soft tissue and bone demarcation at the vertebral pedicles. The relevant vertebral body was identified by counting upward from the sacrum and confirmed by counting the rib levels superiorly and inferiorly. For the pedicle to be measured, the local axial viewing plane (Fig. 1) was adjusted to be

parallel to the superior and inferior endplates of the vertebrae in question (Red line in Fig. 1C) and aligned with the pedicle axis (Red line in Fig. 1B). When the superior and inferior endplate planes were not parallel owing to vertebral wedging, an orientation approximately halfway between (ie, bisecting) the two endplate inclinations was selected. The local sagittal viewing plane (Fig. 1B) then was adjusted such that it was in line with the pedicle axis and perpendicular to the local axial plane (Green line in Fig. 1A). The right pedicle was identified in a similar manner and the local viewing plane orientation again adjusted to be in line with the right pedicle axis in the axial and sagittal viewing planes.

Measurement of Anatomic Landmarks

Anatomic landmarks were identified and measured on each pedicle (Fig. 2). The 3-D coordinates of 17 points (points A through Q) were identified on each pedicle (34 in total for each vertebra), with the appropriate distances and angles between these points (pedicle width, inner cortical pedicle width, pedicle length, chord length, transverse pedicle angle, pedicle height, inner cortical pedicle height, sagittal pedicle angle) calculated from the landmark locations (Fig. 2). These measurement definitions are similar to those described in the literature [7, 16, 18, 31], however we have taken measurements with the coronal, sagittal, and axial planes oriented to better represent the anatomic axes of the pedicle.

Anatomic Measurements

All measurements were completed by one researcher (CMD). Three scans (totaling 40 pedicles) then were selected at random and measured a second time (CMD) to calculate the intraobserver variability. The same three scans then were measured by another of the authors (CAG) to assess the interobserver measurement variability.

The data were grouped to correspond to the anatomic spinal level (T1–T12) of the pedicle being measured, and normalized to the apex of the major curve. With respect to the latter, the apex was designated as level zero, rostral levels given sequential positive values, and caudal levels given sequential negative values. Where the major curve apex was between two vertebral levels (a disc), it was designated the superior of the two levels (an apex at T7–T8 was designated to be T7). A Shapiro-Wilk test indicated the samples did not follow a normal distribution therefore the Wilcoxon matched-pairs signed-rank test with a significance level less than 0.05 was used to compare the

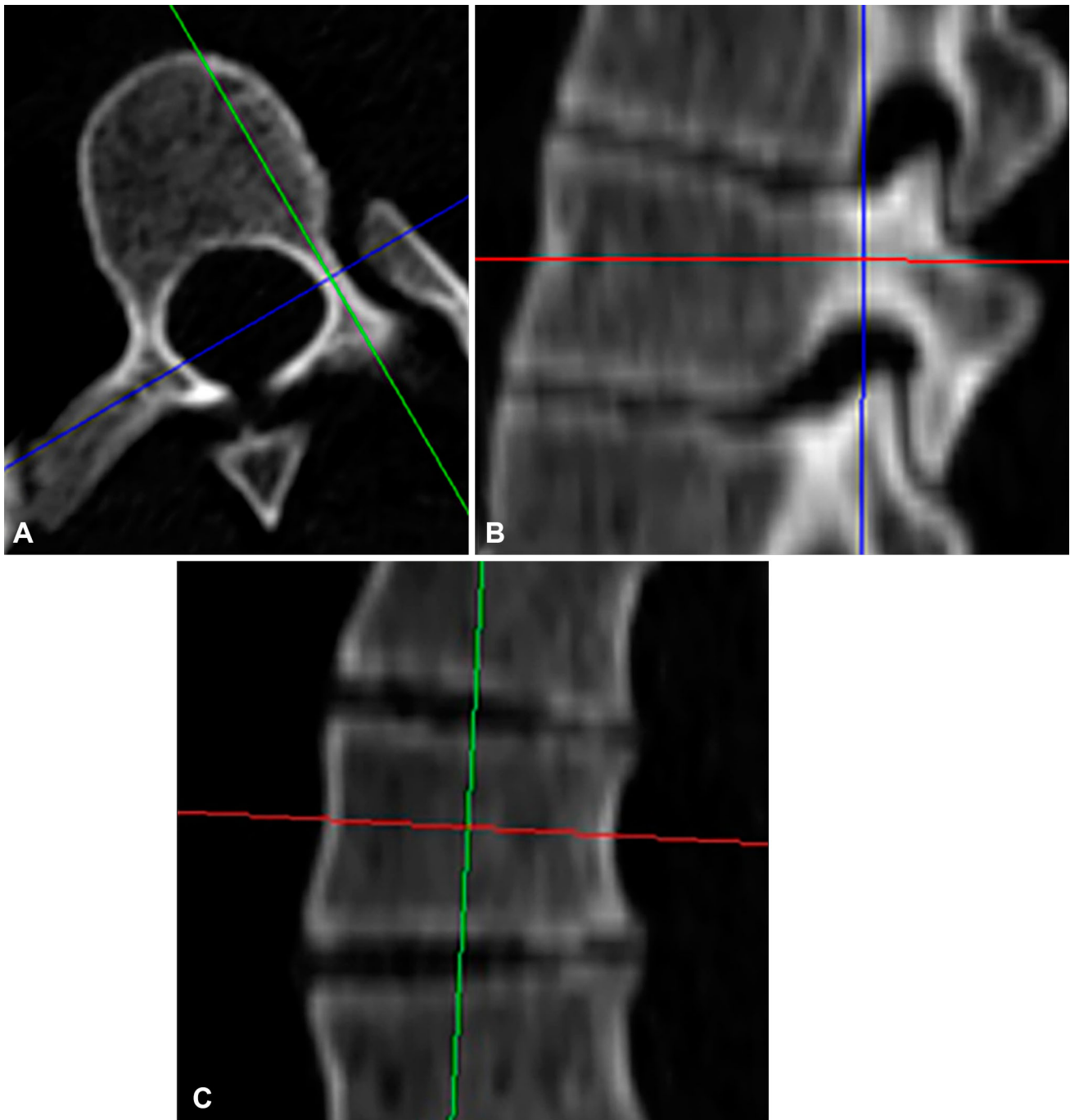


Fig. 1A–C The local (A) axial viewing plane with a sagittal slice (green line) in line with the pedicle axis, (B) sagittal viewing plane with an axial slice (red line) in line with the pedicle axis, and (C)

coronal viewing plane with an axial slice (red line) approximately parallel to the superior and inferior endplates are shown.

morphologic features of the concave and convex pedicles. A similar approach was used by Liljenqvist et al. [18]. Intra- and interobserver errors were evaluated using the mean difference and a 95% limit of agreement analysis was performed following steps outlined by Bland and Altman [3]. Statistical analysis was performed using SPSS Version 22.0 (IBM Corp, Armonk, NY, USA).

Results

Pedicle Anatomy

Asymmetry was identified between the concave and convex pedicles in the axial and sagittal planes. The mean concave pedicle width was smaller than the mean convex

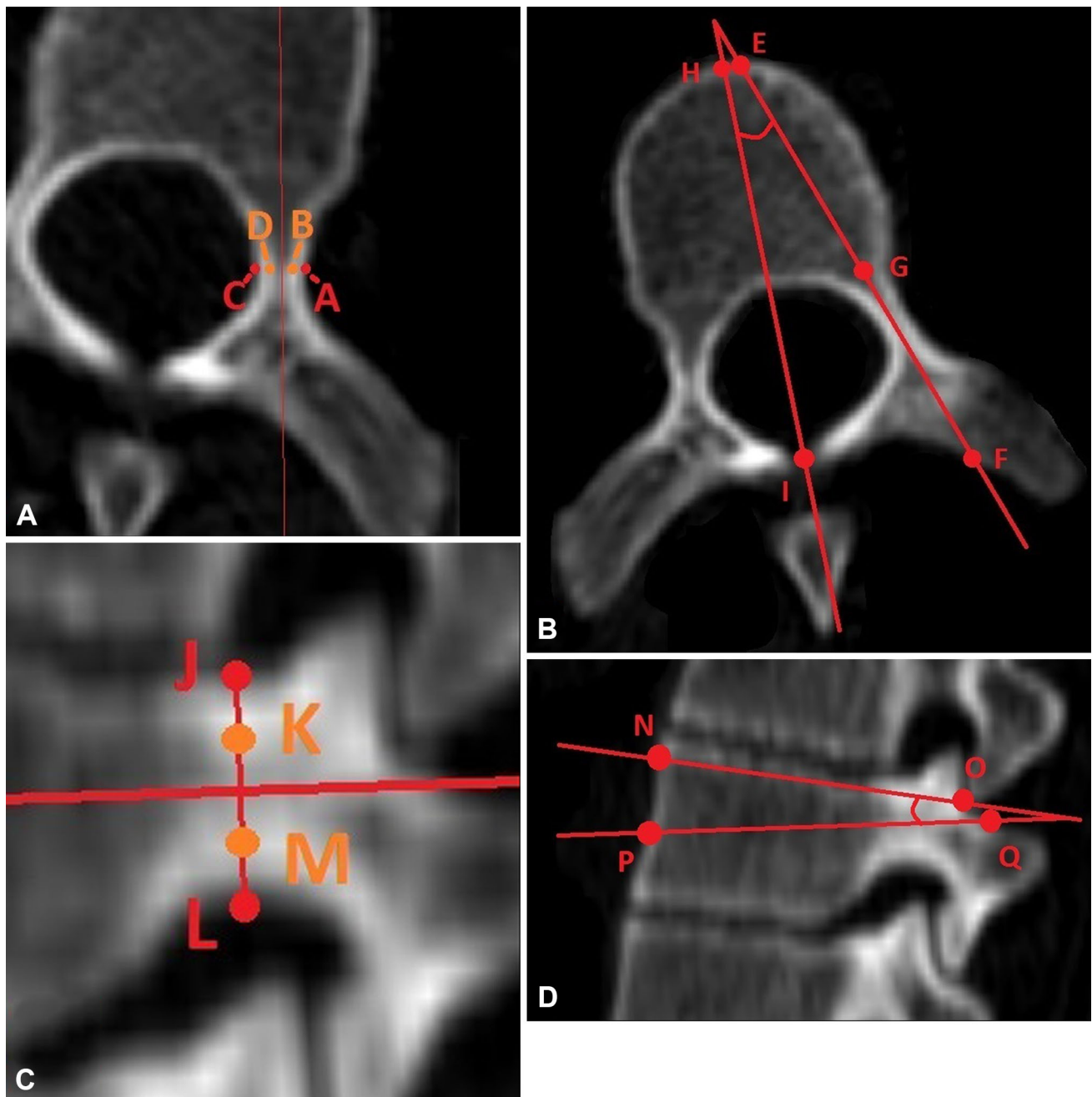


Fig. 2A–D (A) This CT scan of a thoracic vertebrae in the local axial plane shows the outer cortical pedicle width (AC) and the inner cortical pedicle width (BD), where A is the lateral outer cortex margin, B is the lateral inner cortex margin, C is the medial outer cortex margin, and D is the medial inner cortex margin. (B) This scan of a thoracic vertebrae in the local axial plane shows chord length (EF), pedicle length (FG), and transverse pedicle angle (angle between EG and HI), where E is the anterior edge of the vertebral body along the pedicle axis, F is the posterior edge of the vertebra along the pedicle axis, G is a point in line with the posterior longitudinal ligament along the pedicle axis, H is the sagittal midvertebral line at the anterior aspect of the vertebral body, and I is the sagittal midvertebral line at the meeting of the laminae. (C) This

CT scan of a thoracic vertebrae in the local sagittal plane shows the pedicle height (JL) and inner cortical pedicle height (KM), where J is the superior outer cortex margin, K is the superior inner cortex margin, L is the inferior outer cortex margin, and M is the inferior inner cortex margin. (D) This scan of a thoracic vertebrae in the local sagittal plane shows the sagittal pedicle angle (angle between the line NO and PQ), where NO is a line between the anterior (N) and posterior (O) aspects of the vertebrae angled midway between the superior and inferior endplates angles, while PQ is a line between the anterior (P) and posterior (Q) edges of the vertebrae along the pedicle axis in the sagittal viewing plane.

pedicle width around the apex of the curve (T7: 3.44 mm ± 1.16 mm vs 4.72 mm ± 1.02 mm; p < 0.001; mean difference, 1.27 mm; 95% CI, 0.92 mm–1.62 mm); (T8: 3.66 mm ± 1.00 mm vs 4.82 mm ± 1.10 mm; p < 0.001; mean difference, 1.16 mm; 95% CI, 0.84 mm–1.49 mm); (T9: 4.10 mm ± 1.57 mm vs 5.12 mm ± 1.17 mm; p < 0.001; mean difference, 1.02 mm; 95% CI, 0.66 mm–1.39 mm); (T10: 4.79 mm ± 1.57 mm vs 5.34 mm ± 1.27 mm; p = 0.02; mean difference, 0.56 mm; 95% CI, 0.11 mm–1.01 mm) (Fig. 3) with symmetry restored at the rostral and caudal aspects of the major curve (T4–T6 and T11–T12) (Supplemental Table 1. Supplemental material is available with the online version of *CORR*[®]). The pedicle length steadily shortened from T4 to T10 before lengthening again from T10 to T12, however there were no clinically relevant differences noted between the concave and convex sides (Supplemental Table 1. Supplemental material is available with the online version of *CORR*[®]). The chord length on the convex and concave sides increased in size from the rostral to the caudal end of the major curve. The chord length on the concave side was larger than the convex side from T8 to T10 (T8: 39.30 mm ± 3.96 mm vs 37.88 mm ± 3.86 mm; p = 0.031; mean difference, 1.42 mm; 95% CI, 0.26 mm–2.58 mm); (T9: 39.70 mm ± 3.42 mm vs 37.88 mm ± 3.33 mm; p = 0.024; mean difference, 1.80 mm; 95% CI, 0.59 mm–3.01 mm); (T10: 39.17 mm ± 2.39 mm vs 37.33 mm ± 3.06 mm; p = 0.031; mean difference, 1.84 mm; 95% CI, 0.31 mm–3.36 mm) (Supplemental Table 1. Supplemental material is available with the online version of *CORR*[®]). The concave transverse pedicle angle was larger than the convex side from T6 to T9 (T6: 11.37° ± 4.48° vs 8.82° ± 4.31°; p = 0.004; mean difference, 2.54°; 95% CI, 1.10°–

3.99°); T7: 12.69° ± 5.93° vs 8.65° ± 3.79°; p = 0.002; mean difference, 4.04°; 95% CI, 1.90°–6.17°); (T8: 13.24° ± 5.28° vs 7.66° ± 4.87°; p < 0.001; mean difference, 5.58°; 95% CI, 2.99°–8.17°); (T9: 19.95° ± 5.69° vs 8.21° ± 4.02°; p < 0.001; mean difference, 4.74°; 95% CI, 2.68°–6.80°) (Fig. 4). The concave pedicle height was smaller than the convex pedicle height from T5 to T8 (T5: 9.43 mm ± 0.98 vs 10.63 mm ± 1.10 mm; p = 0.002; mean difference, 1.02 mm; 95% CI, 0.59 mm–1.45 mm); T6: 8.87 mm ± 1.37 mm vs 10.88 mm ± 0.81 mm; p <

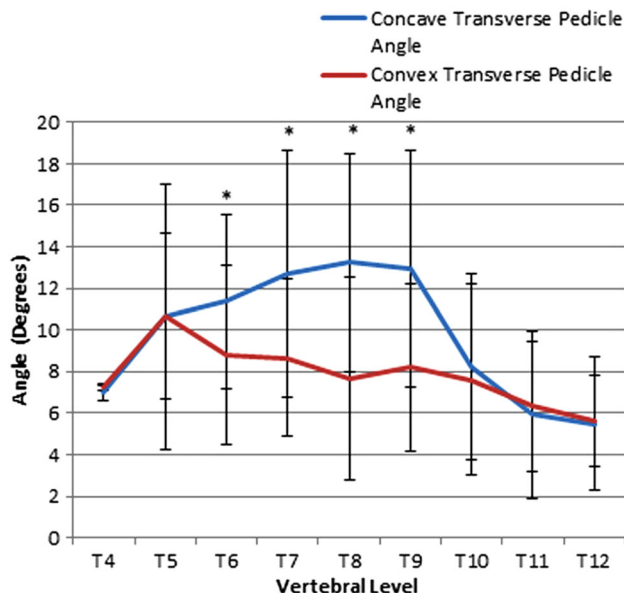


Fig. 4 A comparison of the concave and convex transverse pedicle angles is shown. Error bars = ± 1 SD; *significance of p < 0.05.

Fig 3 The graph shows a comparison of the mean concave and convex pedicle widths and inner pedicle widths at each anatomic vertebral level for the entire patient group (n = 22). Error bars = ± 1 SD; *significance of p < 0.05.

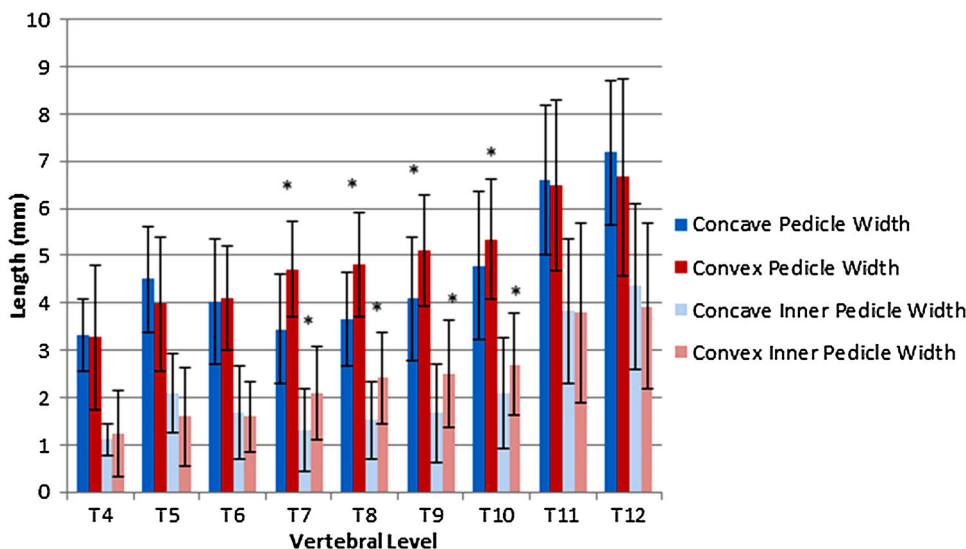
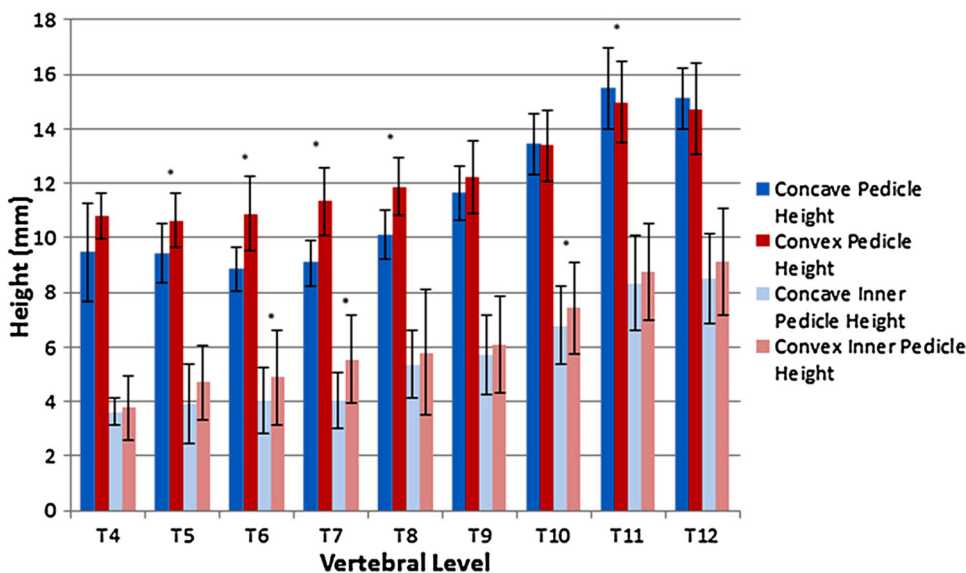


Fig. 5 A comparison of the concave and convex pedicle heights and inner pedicle heights at each anatomic vertebral level is shown. Error bars = ± 1 SD; *significance of p < 0.05.



0.001; mean difference, 2.02 mm; 95% CI, 1.40 mm–2.63 mm); (T7: 9.09 mm ± 1.24 mm vs 11.35 mm ± 0.84 mm; p < 0.001; mean difference, 2.26 mm; 95% CI, 1.81 mm–2.72 mm); (T8: 10.11 mm ± 1.05 mm vs 11.86 mm ± 0.88 mm; p < 0.001; mean difference, 1.75 mm; 95% CI, 1.30 mm–2.19 mm) (Supplemental Table 2. Supplemental material is available with the online version of *CORR*®). Comparatively the concave inner pedicle height was smaller than the convex pedicle height at T6 (4.03 mm ± 1.86 mm vs 4.88 mm ± 1.20 mm; p = 0.042; mean difference, 0.85 mm; 95% CI, 0.02 mm–1.68 mm), T7 (4.04 mm ± 1.62 mm vs 5.55 mm ± 1.03 mm; p < 0.001; mean difference, 1.51 mm; 95% CI, 0.93 mm–2.10 mm); and T10 (6.80 mm ± 1.68 mm vs 7.43 mm ± 1.45 mm; p = 0.039; mean difference, 0.63 mm; 95% CI, 0.07 mm–1.19 mm) (Fig. 5). The concave sagittal pedicle angles were larger than the convex at the levels of T9 (10.83° ± 3.02° vs 8.7° ± 2.91°; p = 0.010; mean difference, 2.13°; 95% CI, 0.79°–3.47°), T10 (10.76° ± 3.71° vs 8.23° ± 3.81°; p = 0.002; mean difference, 2.53°; 95% CI, 1.12°–3.94°), and T12 (7.03° ± 2.19° vs 5.15° ± 1.87°; p = 0.015; mean difference, 1.73°; 95% CI, 0.65°–2.81°) (Fig. 6).

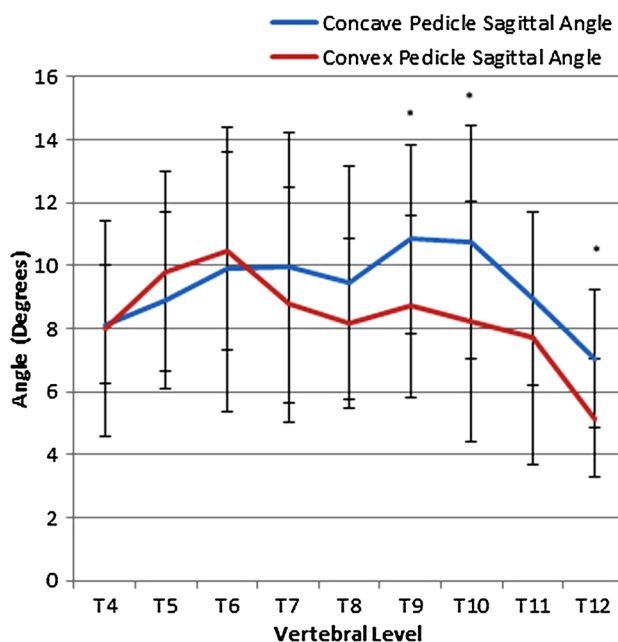


Fig. 6 A comparison of the concave and convex pedicle sagittal angle at each anatomic vertebral level is shown. Error bars = ± 1 SD; *significance of p < 0.05.

Inter- and Intraobserver Variability

Bland-Altman plots showed minimal biases between the two researchers’ measurements. Pedicle width measurements were the most consistent measurements in the intra- and interobserver measurements with 95% limits of agreement of 0.7 mm and 0.8 mm respectively and mean difference of 0.09 mm and 0.18 mm respectively (Table 3). The 95% limit of agreement values were the most variable with the transverse pedicle angles (intraobserver, 4.6°,

mean difference, 0.28°; interobserver, 7.2°, mean difference, 1.12°) and sagittal pedicle angles (intraobserver, 5.9°, mean difference, 1.36°; interobserver, 7.5°, mean difference, 1.50°).

Discussion

When performing pedicle screw instrumentation surgery, inadequate understanding of the pedicle anatomy can result

Table 3. 95% limits of agreement for intra- and interobserver measurement variability

Measurement	Intraobserver 95% limit of agreement (1.96 × SD)	Interobserver 95% limit of agreement (1.96 × SD)
Pedicle width (mm)	0.7	0.8
Inner pedicle width (mm)	1.1	1.1
Chord length (mm)	4.7	5.2
Pedicle length (mm)	4.0	3.8
Transverse pedicle angle (°)	4.6	7.2
Pedicle height (mm)	1.0	1.4
Inner pedicle height (mm)	2.0	2.0
Sagittal pedicle angle (°)	5.9	7.5

in incorrect pedicle screw size and length selection and screw insertion trajectory. These errors could result in pedicle wall expansion or fracture or anterior cortex breach, all of which could result in neurovascular injury or loss of secure fixation [15, 32]. In adolescent idiopathic scoliosis, where the anatomy is three-dimensionally asymmetrically distorted and the pedicles known to at times encroach closer to the spinal cord and aorta [16, 32], it is vital to have an understanding of the morphologic features of the pedicle in all planes. While the pedicle width has been investigated in previous studies using various methods [8, 9, 16, 18, 30, 33, 36], there are clear knowledge gaps or inconsistencies when examining the remaining pedicle parameters. The current study identified clinically relevant asymmetry in the width, height, and angulation of the pedicle in multiple planes using a more clinically relevant and reliably reproducible measurement technique. Smaller pedicle widths and heights and larger pedicle angles on the concave side of the curve were identified when compared with the convex side around the apex of the curve.

Although the dataset used in this study was captured from patients undergoing anterior thoracoscopic surgical correction, a posterior correction using pedicle screws also would be an appropriate treatment protocol, therefore the subjects were considered to be a relevant cohort for this investigation. The inclusion criteria were set to provide as much consistency as possible in the dataset without limiting the cohort size. While a previous study looking at spinal anatomy showed no difference between males and females [30], with only one male in the dataset, we elected to exclude this male patient. Similarly we excluded the one curve which extended to L1 with an apex at T10, as it was thought this curve type may skew results, considering the most clinically relevant findings were found periapically. Owing to the limited cohort size, age, skeletal maturity, and race were not able to be subcategorized. Race can

affect absolute pedicle size, with anatomic studies in Japanese [28] and Indian [30] patients with adolescent idiopathic scoliosis showing smaller absolute pedicle sizes compared with a western population.

Although direct measurement using cadaveric specimens is the gold standard for anatomic studies, sourcing adolescent cadavers with spinal deformities of operable severity and of sufficient numbers is not feasible. However, CT scans have been shown to have good correlation with direct measurement using cadaveric specimens for anatomic measurements of spinal anatomy [13, 20]. The use of a control group would have been beneficial but performing CT scans on healthy age-matched subjects for research purposes is ethically unacceptable owing to radiation exposure. While CT scans are currently not routinely conducted preoperatively, one still can adapt these findings to their intraoperative imaging and procedures.

Pedicle width, being the smallest cross-sectional dimension, is the most important factor as it dictates the maximum pedicle screw diameter that can be accommodated safely without medial or lateral cortical breach. Our study showed clinically relevant smaller pedicle widths (inner and outer cortical) on the concave side periapically—a finding consistent with previous studies using CT, MRI, and cadavers [1, 18, 21, 25, 30, 35]. Inner and outer cortical pedicle widths were measured to provide clarity over the inconsistencies or ambiguities that existed in the measurement definitions in previous studies [9, 36]. With the chord length being longer on the concave side of the curve at T8–T10, but no difference seen in the pedicle lengths, it can be inferred that the length from the anterior cortex of the vertebral body to the anterior aspect of the pedicle along the pedicle axis is longer on the concave side. It has been proposed with the rotational deformity, the vertebral body veers toward the concavity in the transverse plane which results in a longer chord length on the concave side [37]. Although statistically different, clinically it only translates into an absolute difference of between 1.4 to 1.8 mm. While pedicles with a mild ‘windswept’ pedicle were observed during the measurement phase, they did not affect pedicle length. However, they may explain the increase seen in the transverse pedicle angles on the concave side around the apex of the curve. In normal spines without deformity, the transverse pedicle angle gradually decreases from T1 to T12 before increasing again in the lumbar spine [7, 31, 37]. While the rostral and caudal ends of the curve in the patients in this study were consistent with those reported in previous studies [5, 16, 18], only one of these previous studies [16] followed the trend seen in our study while the other two [5, 18] did not identify any difference between the two sides of the curve. It is thought the differences seen in the transverse pedicle angles is attributable to intravertebral

rotation [16]. The definition of the sagittal pedicle angle varies among studies [5, 7, 36, 37]. We used a modified version of the definitions reported by Ebraheim et al. [7], as it was deemed the most clinically applicable angle for pedicle screw insertion.

In the literature, only two previous studies have measured intraobserver error [16, 18], whereas to our knowledge, no prior study has investigated interobserver error. Angular measurements, clinically translated to the trajectory of the pedicle screw, had the most variation in our study (95% limits of agreement in the range of 5° to 7° for transverse and sagittal pedicle angles), a finding also noted in the two previous studies [16, 18]. Reasons for this appear to be multifactorial with interstudy variation being contributed to by the disparity in angular measurement definitions, while intrastudy variation can be at least partially attributed to scan limitations. With the maximal in-plane pixel thickness of 0.78 mm and maximum CT slice thickness of 1.25 mm we used, a single pixel difference in selecting an anatomic landmark can result in as much as 1.93° angulation difference when measuring the transverse pedicle angle using an average chord length (1.25 mm / 37 mm × tan⁻¹ = 1.93°). While the linear measurements were more robust, like the angular measurements, one needs to take into account that the reproducibility of linear measurements also is bounded by the longest voxel dimension in the CT scan (1.25 mm in this case). These factors were not taken into account in the previous studies looking at variability [16, 18].

The morphologic features of the pedicles in patients with adolescent idiopathic scoliosis show a distinct asymmetric intravertebral deformity, which is most pronounced around the apical region of the major thoracic curve. Specifically the concave pedicles were found to be smaller in diameter in the axial and sagittal planes and more medially directed compared with the convex side. Identifying these clinically relevant differences provides important pedicle screw size and trajectory information for surgeons during corrective scoliosis surgery. Based on the results of the current study which analyzed thoracic vertebral levels, and taking into consideration the above factors, one could advocate the use of 3.5 mm diameter screws for levels T5 to T9 and 4.5 mm screws for levels T10 to T12. These findings are similar to the recommendations of Catan et al. [5] who recommended 3.5 mm screws for T3 to T9 and 4.5 mm screws for T9 to T12.

We acknowledge that CT scans no longer are routinely performed preoperatively, and as such, we propose future studies use MRI to examine different patient groups or curve types and severities.

Acknowledgments We thank the High-Performance Computing and Research Support group at Queensland University of Technology for the computational resources and services used in this work.

Although no project funds were received for this work, the authors wish to acknowledge the group operating support provided by DePuy Synthes Spine, Medtronic, and the Mater Foundation.

References

1. Abul-Kasim K, Ohlin A. Patients with adolescent idiopathic scoliosis of Lenke type-I curve exhibit specific pedicle width pattern. *Eur Spine J.* 2012;21:57–63.
2. Barr SJ, Schuette AM, Emans JB. Lumbar pedicle screws versus hooks: results in double major curves in adolescent idiopathic scoliosis. *Spine (Phila Pa 1976).* 1997;22:1369–1379.
3. Bland JM, Altman DG. Applying the right statistics: analyses of measurement studies. *Ultrasound Obstet Gynecol.* 2003;22:85–93.
4. Boos N, Webb JK. Pedicle screw fixation in spinal disorders: a European view. *Eur Spine J.* 1997;6:2–18.
5. Çatan H, Buluç L, Anik Y, Ayyıldız E, Şarлак AY. Pedicle morphology of the thoracic spine in preadolescent idiopathic scoliosis: magnetic resonance supported analysis. *Eur Spine J.* 2007;16:1203–1208.
6. Cobb J. Outline for the study of scoliosis. In: Edwards J, ed. *Instructional Course Lectures.* Vol 5. Ann Arbor, MI: American Academy Orthopaedic Surgery; 1948:261–275.
7. Ebraheim NA, Xu R, Ahmad M, Yeasting RA. Projection of the thoracic pedicle and its morphometric analysis. *Spine (Phila Pa 1976).* 1997;22:233–238.
8. Halm H, Niemeyer T, Link T, Liljenqvist U. Segmental pedicle screw instrumentation in idiopathic thoracolumbar and lumbar scoliosis. *Eur Spine J.* 2000;9:191–197.
9. Hu X, Siemionow KB, Lieberman IH. Thoracic and lumbar vertebrae morphology in Lenke type 1 female adolescent idiopathic scoliosis patients. *Int J Spine Surg.* 2014; Dec 1;8. doi: 10.14444/1030.
10. Jutte PC, Castelein RM. Complications of pedicle screws in lumbar and lumbosacral fusions in 105 consecutive primary operations. *Eur Spine J.* 2002;11:594–598.
11. Kamimura M, Kinoshita T, Itoh H, Yuzawa Y, Takahashi J, Hirabayashi H, Nakamura I. Preoperative CT examination for accurate and safe anterior spinal instrumentation surgery with endoscopic approach. *J Spinal Disord Tech.* 2002;15:47–51; discussion 51–52.
12. Kosmopoulos V, Schizas C. Pedicle screw placement accuracy: a meta-analysis. *Spine (Phila Pa 1976).* 2007;32:E111–E120.
13. Krag MH, Weaver DL, Beynon BD, Haugh LD. Morphometry of the thoracic and lumbar spine related to transpedicular screw placement for surgical spinal fixation. *Spine (Phila Pa 1976).* 1988;13:27–32.
14. Lenke LG, Betz RR, Harms J, Bridwell KH, Clements DH, Lowe TG, Blanke K. Adolescent idiopathic scoliosis: a new classification to determine extent of spinal arthrodesis. *J Bone Joint Surg Am.* 2001;83:1169–1181.
15. Li G, Lv G, Passias P, Kozanek M, Metkar US, Liu Z, Wood KB, Rehak L, Deng Y. Complications associated with thoracic pedicle screws in spinal deformity. *Eur Spine J.* 2010;19:1576–1584.
16. Liljenqvist UR, Allkemper T, Hackenberg L, Link TM, Steinbeck J, Halm HF. Analysis of vertebral morphology in idiopathic scoliosis with use of magnetic resonance imaging and multiplanar reconstruction. *J Bone Joint Surg Am.* 2002;84:359–368.
17. Liljenqvist UR, Halm HF, Link TM. Pedicle screw instrumentation of the thoracic spine in idiopathic scoliosis. *Spine (Phila Pa 1976).* 1997;22:2239–2245.
18. Liljenqvist UR, Link TM, Halm HF. Morphometric analysis of thoracic and lumbar vertebrae in idiopathic scoliosis. *Spine (Phila Pa 1976).* 2000;25:1247–1253.

19. Loch-Wilkinson TJ, Izatt MT, Labrom RD, Askin GN, Percy MJ, Adam CJ. Morphometric analysis of the thoracic intervertebral foramen osseous anatomy in adolescent idiopathic scoliosis using low-dose computed tomography. *Spine Deform.* 2016;4:182–192.
20. Misenhimer GR, Peek RD, Wiltse LL, Rothman SL, Widell EH Jr. Anatomic analysis of pedicle cortical and cancellous diameter as related to screw size. *Spine (Phila Pa 1976).* 1989;14:367–372.
21. Parent S, Labelle H, Skalli W, de Guise J. Thoracic pedicle morphometry in vertebrae from scoliotic spines. *Spine (Phila Pa 1976).* 2004;29:239–248.
22. Risser JC. The Classic: The iliac apophysis: an invaluable sign in the management of scoliosis. *Clin Orthop Relat Res.* 2010;468:646–653.
23. Roach JW. Adolescent idiopathic scoliosis. *Orthop Clin North Am.* 1999;30:353–365, vii–viii.
24. Schick D. Computed tomography radiation doses for paediatric scoliosis scans. Brisbane, Australia: Internal report commissioned by QUT Mater Health Services Paediatric Spine Research Group from Queensland Health Biomedical Technology Services; 2004.
25. Smith RM, Pool RD, Butt WP, Dickson RA. The transverse plane deformity of structural scoliosis. *Spine (Phila Pa 1976).* 1991;16:1126–1129.
26. Suk SI, Lee CK, Kim WJ, Chung YJ, Park YB. Segmental pedicle screw fixation in the treatment of thoracic idiopathic scoliosis. *Spine (Phila Pa 1976).* 1995;20:1399–1405.
27. Suk SI, Lee CK, Min HJ, Cho KH, Oh JH. Comparison of Cotrel-Dubousset pedicle screws and hooks in the treatment of idiopathic scoliosis. *Int Orthop.* 1994;18:341–346.
28. Takeshita K, Maruyama T, Chikuda H, Shoda N, Seichi A, Ono T, Nakamura K. Diameter, length, and direction of pedicle screws for scoliotic spine: analysis by multiplanar reconstruction of computed tomography. *Spine (Phila Pa 1976).* 2009;34:798–803.
29. Tian NF, Huang QS, Zhou P, Zhou Y, Wu RK, Lou Y, Xu HZ. Pedicle screw insertion accuracy with different assisted methods: a systematic review and meta-analysis of comparative studies. *Eur Spine J.* 2011;20:846–859.
30. Upendra B, Meena D, Kandwal P, Ahmed A, Chowdhury B, Jayaswal A. Pedicle morphometry in patients with adolescent idiopathic scoliosis. *Indian J Orthop.* 2010;44:169–176.
31. Vaccaro AR, Rizzolo SJ, Allardyce TJ, Ramsey M, Salvo J, Balderston RA, Cotler JM. Placement of pedicle screws in the thoracic spine: Part I: morphometric analysis of the thoracic vertebrae. *J Bone Joint Surg Am.* 1995;77:1193–1199.
32. Vaccaro AR, Rizzolo SJ, Balderston RA, Allardyce TJ, Garfin SR, Dolinskas C, An HS. Placement of pedicle screws in the thoracic spine: Part II: an anatomical and radiographic assessment. *J Bone Joint Surg Am.* 1995;77:1200–1206.
33. Weinstein JN, Rydevik BL, Rauschnig W. Anatomic and technical considerations of pedicle screw fixation. *Clin Orthop Relat Res.* 1992;284:34–46.
34. Weinstein SL, Dolan LA. The evidence base for the prognosis and treatment of adolescent idiopathic scoliosis: the 2015 Orthopaedic Research and Education Foundation Clinical Research Award. *J Bone Joint Surg Am.* 2015;97:1899–1903.
35. Xiong B, Sevastik B, Willers U, Sevastik J, Hedlund R. Structural vertebral changes in the horizontal plane in idiopathic scoliosis and the long-term corrective effect of spine instrumentation. *Eur Spine J.* 1995;4:11–14.
36. Zindrick MR, Knight GW, Sartori MJ, Carnevale TJ, Patwardhan AG, Lorenz MA. Pedicle morphology of the immature thoracolumbar spine. *Spine (Phila Pa 1976).* 2000;25:2726–2735.
37. Zindrick MR, Wiltse LL, Doornik A, Widell EH, Knight GW, Patwardhan AG, Thomas JC, Rothman SL, Fields BT. Analysis of the morphometric characteristics of the thoracic and lumbar pedicles. *Spine (Phila Pa 1976).* 1987;12:160–166.